Algorithm Theoretical Basis Document for the Automatic Satellite Image Interpretation Processors of the NWC/GEO

NWC/CDOP2/GEO/ZAMG/SCI/ATBD/ASII, Issue 1.1

15 October 2016

Applicable to

GEO-ASII-v2.4.1 (NWC-046a)

GEO-ASII-NG-v1.0 (NWC-047)

Prepared by ZAMG

REPORT SIGNATURE TABLE

Function	Name	Signature	Date
Prepared by	A. Wirth & B. Zeiner (ZAMG)		*15 October 2016*
Revised by	A. Wirth (ZAMG)		*15 October 2016*
Reviewed by	R. Goler, A. Jann (ZAMG)		*15 October 2016*
Authorised by	Pilar Rípodas SAFNWC Project Manager		*15 October 2016*

DOCUMENT CHANGE RECORD

Version	Date	Pages	CHANGE(S)
1.0	29 November 2013	15	Initial version, for the SAFNWC/MSG release 2015.
1.1	15 October *2016*	17	Updated version, for the actual NWC/GEO release 2016.

Table of contents

List of Tables and Figures

1. INTRODUCTION

1.1 SCOPE OF THE DOCUMENT

This document is the Algorithm Theoretical Basis Document for the "Automatic Satellite Image Interpretation – Next Generation" (ASII-NG) / PGE 17 of the NWC/GEO software package. Note that unlike other documentation of the NWC/GEO Met.Systems suite, this one does not include information on the "Automatic Satellite Image Interpretation" (ASII) / PGE 10, as the ATBD for this product (SAF/NWC/CDOP2/ZAMG/SCI/ATBD/10) is kept separated for readability considerations and because of the "scientifically frozen" status of that PGE which implies that the ATBD undergoes no change.

This document contains a description of the algorithms, including scientific aspects and practical considerations.

1.2 SOFTWARE VERSION IDENTIFICATION

This document describes the algorithms implemented in the PGE 17 version 1.0 included in the 2016 NWC/GEO software package delivery, and those envisaged for a release in 2018, for which a prototype has already been developed.

1.3 IMPROVEMENTS SINCE THE PREVIOUS RELEASE

The new version reflects the actual status at the time of the release of NWC/GEO v2016.

1.4 DEFINITIONS, ACRONYMS AND ABBREVIATIONS

ASII	Automatic Satellite Image Interpretation
ASII-NG	ASII next generation
BT	Brightness Temperature
CAT	clear air turbulence
HRV	High Resolution Visible
HRW	High Resolution Winds
IR	infrared
NWP	Numerical Weather Prediction
PIREP	Pilot Report
PVA	positive vorticity advection
REF	Reflectivity
SEVIRI	Spinning Enhanced Visible and Infra-Red Imager
VIS	visible
WV	water vapour
ZAMG	Zentralanstalt für Meteorologie und Geodynamik

1.5 REFERENCES

1.5.1 Applicable Documents

The following documents, of the exact issue shown, form part of this document to the extent specified herein. Applicable documents are those referenced in the Contract or approved by the Approval Authority. They are referenced in this document in the form [AD.X]

For dated references, subsequent amendments to, or revisions of, any of these publications do not apply. For undated references, the current edition of the document referred applies.

Current documentation can be found at the NWC SAF Helpdesk web: http://www.nwcsaf.org.

Ref	Title	Code	Vers	Date
[AD.1]	Proposal for the Second Continuous Development and Operations Phase (CDOP) March 2012 – February 2017	NWC/CDOP2/MGT/AEMET/PRO	1.0d	15/03/11
[AD.2]	NWCSAF Project Plan	NWC/CDOP2/SAF/AEMET/MGT/PP	1.9	15/10/16
[AD.3]	Configuration Management Plan for the SAFNWC/GEO	NWC/CDOP2/GEO/AEMET/MGT/CMP	1.4	15/10/16
[AD.4]	NWCSAF Product Requirements Document	NWC/CDOP2/SAF/AEMET/MGT/PRD	1.9	15/10/16
[AD.5]	System and Components Requirements Document for the NWC/GEO	NWC/CDOP2/GEO/AEMET/SW/SCRD	1.2	15/10/16

Table 1: List of Applicable Documents

1.5.2 Reference Documents

The reference documents contain useful information related to the subject of the project. This reference document complements the applicable documents. For dated references, subsequent amendments to, or revisions of, any of these publications do not apply. For undated references, the latest edition of the document referred to applies.

Latest documentation can be found at the SAFNWC Help Desk at http://www.nwcsaf.org

Reference	Title	Code	Vers	Date
[RD.1]	Data Output Format of the SAFNWC/GEO	NWC/CDOP2/GEO/AEMET/SW/DOF	1.2	
[RD.2]				
[RD.3]				

Table 2: List of Referenced Documents

2. AREAS WITH RISK OF CAT – OVERVIEW

During the precedent phases of NWCSAF, the Automatic Satellite Image Interpretation (ASII) product has been developed to analyse satellite imagery in terms of conceptual models of atmospheric phenomena, e.g. cold fronts, warm fronts, dry intrusions, etc. It came to a point that the conceptual model method could no longer be improved, and so it was decided in the "Next-Generation" (NG) product to employ a new method of analysis to detect features in satellite data. This method will be used to investigate other features which are of great interest to meteorologist and/or further users. One of these features is clear air turbulence (CAT), which is of importance to aviation, and will be discussed in some detail on the following pages.

Clear-air turbulence is non-convective turbulence outside the planetary boundary layer, often in the upper troposphere. CAT typically has a patchy structure and horizontal dimensions of 80-500 km in the along-wind direction and 20-100 km in the across-wind direction. Vertical dimensions are 500-1000 m, and the lifespan of CAT is between half an hour and a day (Overeem, 2002). Forecasts of CAT in numerical weather models are difficult to perform because the scale of the physical processes involved in turbulence are smaller than most model resolutions. Furthermore, verification is problematic since pilot reports are subjective (although there are airplanes with instruments measuring vertical acceleration) and unevenly distributed. Thus it is of interest here to develop a method to at least identify areas from satellite data which show (high) risks of CAT.

As its name suggests, CAT cannot be observed directly from satellite imagery since it occurs in cloud free regions. However, there exist several indicators in the vicinity of a region of CAT which can be observed in satellite data which provide an indication that CAT is likely to occur.

3. ALGORITHM DESCRIPTION

3.1 THEORETICAL DESCRIPTION

3.1.1 Physics of the problem

The role of ASII-NG is to detect regions of turbulence based on meteorological parameters and combinations thereof that are indicators of turbulence.

In general, CAT occurs preferentially in the following meteorological situations:

- Tropopause folds
- Gravity waves (e.g. lee waves)
- Air mass boundaries (e.g. fronts)
- Wind shear (e.g. jets)
- Convection

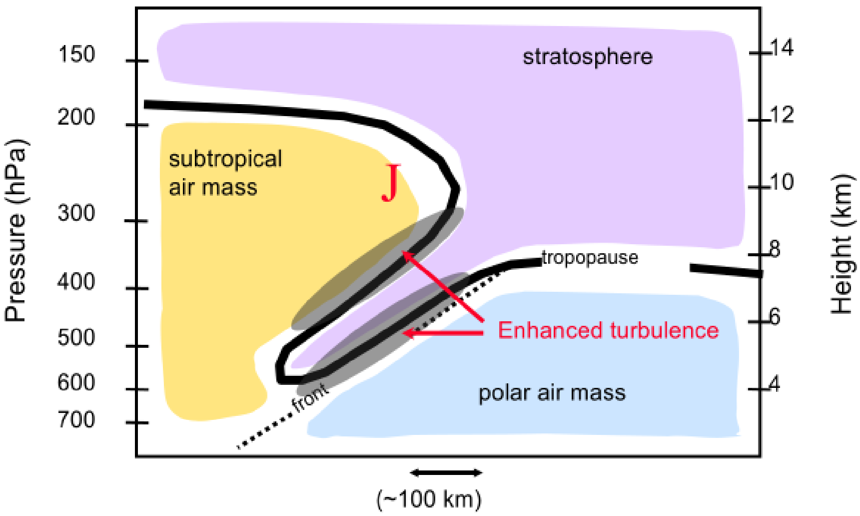

Figure 1: Schematic of a tropopause fold[1].

A tropopause fold describes the downward intrusion of stratospheric air into the troposphere which results in a "folding" of the tropopause, as schematically illustrated in Figure 1. Typically at a tropopause fold there is the vertical shearing at the jet stream combined with the ageostrophic convergence of polar, subtropical, and stratospheric air masses. Tropopause folds mark the change in the height of the tropopause and are characterized by the occurrence of strong turbulence. Stratospheric air, which characteristically has a low moisture content and a high potential vorticity can protrude down to the mid or even the lower troposphere. Consequently, tropopause folds can be located by their association with gradients in upper level moisture, which are evident in the SEVIRI 6.2 µm channel sensitive to upper tropospheric water vapour. A tropopause folding turbulence product based on the ABI (Advanced Baseline Imager) sensor flown on the GOES-R series of NOAA geostationary meteorological satellites and using the 6.1 µm channel has been developed by NOAA NESDIS (Wimmers and Feltz, 2010). The tropopause

---

[1] Schematic courtesy of Feltz and Wimmers, 2010: "GOES-R AWG Aviation Team: Tropopause Folding Turbulence Prediction (TFTP)"

height can be determined from NWP parameters such as the temperature, specific humidity or potential vorticity. The ozone content derived from SEVIRI IR channel at 9.7 µm is a good indicator for the presence of a tropopause fold. The lower the tropopause the more ozone is sensed by the SEVIRI instrument onboard MSG satellites. Air mass boundaries, which often coincide with tropopause folds, can be determined from satellite data. Transition zones between polar and tropical air masses are reflected in the MSG "ozone channel" IR 9.7 µm.

In the lee of mountain ridges, turbulence occurs below lee waves where a rotor cloud can develop. The turbulence cannot be directly seen, but mountain waves show the typical pattern of parallel white lines aligned perpendicular to the wind direction. Two kinds of lee waves can be discriminated: trapped lee waves which are bound to a certain layer (due to stratification they cannot propagate across an "upper" and a "lower" border) and non-trapped lee waves which are propagating both in vertical and horizontal directions. The energy balance is different for those two cases. For the trapped lee waves the energy of the waves is conserved within the layer – with an exchange of energy from non-turbulent to turbulent flow, whereas in the latter case energy can be transported vertically.

One criterion to estimate turbulence is the existence of a foehn gap between mountain ridge and lee clouds (Ellrod and Knox, 2010). In the case of turbulence, a pronounced sinking zone can be seen in WV, VIS and IR images. There also exists a correlation between wave length and turbulence intensity. In addition, the intensity of turbulence may be assessed by the complexity of the cloud pattern; the more complex the pattern is (e.g. crossing wave fronts) then the higher the intensity of turbulence (Uhlenbrock et al., 2007). However, these factors can probably be applied only to a very limited extent in an automatic detection tool.

Although lee clouds can be expected behind large surface elevations like mountain ranges or elevated coasts, they can also occur in lee of small hills or islands. Important for the formation of lee waves is the angle between the main wind direction and the orientation of the mountain range, and the stability of the layer of air. Ideal conditions for the appearance of lee waves occur when the air flow is near to perpendicular to the surface elevation. The wind speed ideally should exceed a certain value to allow the air flow to overflow the mountain range rather than to circulate around. In case of mountain heights up to 1000 m the wind speed should be larger than 8-10 m/s, while for higher mountain ranges, a wind speed of more than 12-15 m/s is necessary (World Meteorological Organization, 1978). An increase of the wind speed up to 20-25 m/s has shown beneficial for the development of lee waves. Lee wave development ideally occurs when the wind direction is constant with height, although variations up to 20°/ 1000m do not affect their development.

At the edge of polar fronts and in the cirrus plume associated with subtropical jets, transverse cloud bands can sometimes be observed in the IR satellite images. Turbulence at jet level originates from large vertical wind shear (Bader et al. 1995). Friction among layers with varying wind speed leads to the formation of small scale eddies (Kelvin-Helmholtz instability). Transversal cloud bands are a good indicator of turbulence at jet level.

In cases where a thermal inversion separates two layers with a marked difference in wind direction and/or speed (i.e. wind shear), gravity waves may be produced. If the wind encounters distortions at the inversion layer caused by thermals coming up from below, it will create significant shear waves in the lee of the distortions.

Turbulence is closely related to convection. Vertical mass exchanges lead to up- and downdrafts causing turbulence. However, ASII-NG intentionally does not deal with the detection of convective cells as this topic is covered elsewhere in the NWCSAF portfolio.

Algorithms developed previously to predict/analyse the occurrence of CAT were primarily based on NWP output (Elrod and Knapp, 1991), not taking into account information provided by satellite sensors. A typical example for a turbulence warning system is the Graphical Turbulence

Guidance (GTG and GTG2), developed by NCAR (Sharman et al., 2004). There currently exist a large number of numerical parameters to diagnose turbulence, but to date an all-encompassing parameter does not exist. For example, potential vorticity is critical to the detection of tropopause folds (Wimmers and Feltz, 2010); PVA is considered to be the leading parameter in the detection of gravity waves associated with jets (transverse bandings; Knox et al., 2007); vorticity and upper level divergence are considered relevant for transverse bandings at the outflow of thunderstorms (Lenz, 2008). When considering mountain waves, characteristic numbers describing the flow, and layer stability, e.g. the Richardson Number (McCann, 2001), or some special indices developed for classifying turbulence (Ellrod Index, Brown Index, Dutton Index) are the most important measures of turbulence (Overeem, 2002). When using NWP data, the resolution of the model is crucial since turbulence is a small-scale phenomenon and is not resolved by common operational models.

3.1.2 Mathematical description of the algorithm

3.1.2.1 Logistic regression

Ideally, the outcome of a subjective image interpretation with respect to a certain phenomenon is a binomial one, segregating the image into areas of “present” (=1) and “not present” (=0). The parameters used to arrive at that conclusion are typically continuous. A logistic regression is a possible framework to formalize that situation in a mathematical model required to attempt automatic image interpretation. As in an ordinary multiple regression, we have a dependent variable Y and several independent variables X_i tied together in a linear combination. However, the governing equation in logistic regression is somewhat more complex in order to account for the dichotomous nature of the predictand Y (P is the probability that Y=1):

$$\ln[P/(1-P)]=b_0+b_1X_1+b_2X_2+b_3X_3...$$

In order to establish the regression relation, test samples had to be collected. A sample size of 30 scenes was used, where a meteorologist subjectively encircled the regions where the phenomenon in question seemed to be present. Providing these analyses and the predictands X_i for the respective scenes, regression coefficients b_i can be deduced through an iterative computation. Once this is achieved, the rest (i.e. the actual derivation of the product) is straightforward: Assemble the input data for the requested slot, compute the variables X_i and derive the probability for the presence of the phenomenon at every pixel (with the above equation solved for P).

3.1.2.2 Detection of tropopause folds

Table 3 shows the input parameters required for the detection of turbulence related to **tropopause folds**. Two heights of the tropopause [hPa] are calculated from the NWP data – one based on specific humidity, and the other based on potential vorticity. For both tropopause heights, it is the gradient field that serves as input into the logistic regression. It is recommended that NWP data be provided up to the 50 hPa level to ensure that the tropopause is captured.

Brightness temperature from channels IR 9.7 µm and IR 10.8 µm directly serve as input, yet there are also some post-processed satellite data involved: A smoothing operator is applied twice to each of WV 6.2 µm, IR 10.8 µm and the channel difference (IR 9.7 µm – IR 10.8 µm) before the gradient fields are calculated. These gradient fields are then input into the logistic regression relation.

NWP parameter	Satellite data
specific humidity	WV 6.2 µm
potential vorticity	IR 9.7 µm

absolute value of shear vorticity at 300 hPa	IR 10.8 µm
wind speed at 300 hPa	

Table 3: Input parameters from NWP and satellite data for the detection of tropopause folds

3.1.2.3 Detection of gravity waves

For mountain waves and transversal bandings a method had to be implemented which can detect parallel cloud bands on meso-gamma (2-20 km) to meso-beta (20-200 km) range. The difference between both types (in the sense of pattern recognition) is the circumstance that transverse banding occurs at the edge of (frontal) cloud bands at jet level while mountain waves typically appear in the low to mid troposphere and are independent of other cloud features. However, there are situations where mountain waves are embedded within fronts. An algorithm to detect cloud bands perpendicular to the wind direction (wind direction provided either by NWP output or by HRW derived from satellite data) has been developed at ZAMG[2]. Table 4 shows the input parameters required for the detection of turbulence related to **atmospheric gravity waves (e.g. lee waves).**

NWP parameter	Satellite data	NWCSAF products
wind direction (on main pressure levels)	VIS 0.8 µm	Cloud Top Height
wind speed (on main pressure levels)	IR 10.8 µm	Extrapolated Imagery
Stability index	HRV	

Table 4: Input parameters from NWP and satellite data for the detection of gravity waves

A wind field taken from HRW or from NWP data provides the wind direction on a grid whose resolution is configurable by the user. For the time being, three main sources for the wind speed and direction are implemented in the prototype software:

1. model winds
2. HRW from PGE09 on a non-regular grid
3. Interpolated HRW field from PGE16 on a regular grid

HRW data from PGE09 based on a non-regular grid have shown that wind information is often missing over stationary cloud pattern like lee waves. Preliminary results suggest that a spatially interpolated HRW field, as internally computed by EXIM/PGE16, should be used instead.

At each point of the user configurable grid, a line of certain pixel length is constructed parallel to the local wind direction (Figure 2). Along this line, satellite pixel information (i.e. brightness temperature and reflectivity) are used to calculate statistical parameters like standard deviation, mean pixel value, and highest pixel gradient to determine if the line is located within a wave structure.

This algorithm can be used to detect both types of atmospheric gravity waves (i.e. mountain waves and transverse bandings). As indicated by Table 4, the wave detection algorithm is applied to VIS0.8 µm, IR10.8 µm and HRV image data. In order to have an image resolution between low resolution images (VIS0.8 µm and IR10.8 µm) and the higher resolution HRV image, the latter is slightly degraded in resolution. This is achieved by eliminating every third pixel from the HRV

[2] This module is currently in a prototype software stage and not distributed in NWC/GEO v2016.

data so that the obtained image has 2/3 of the original HRV pixel information. The reason for doing this operation is to submit a wider spectrum of wave scales to the detection algorithm. During the night time hours, satellite input is reduced to the IR10.8 µm channel, and consequently a different logistic regression relation is to be used.

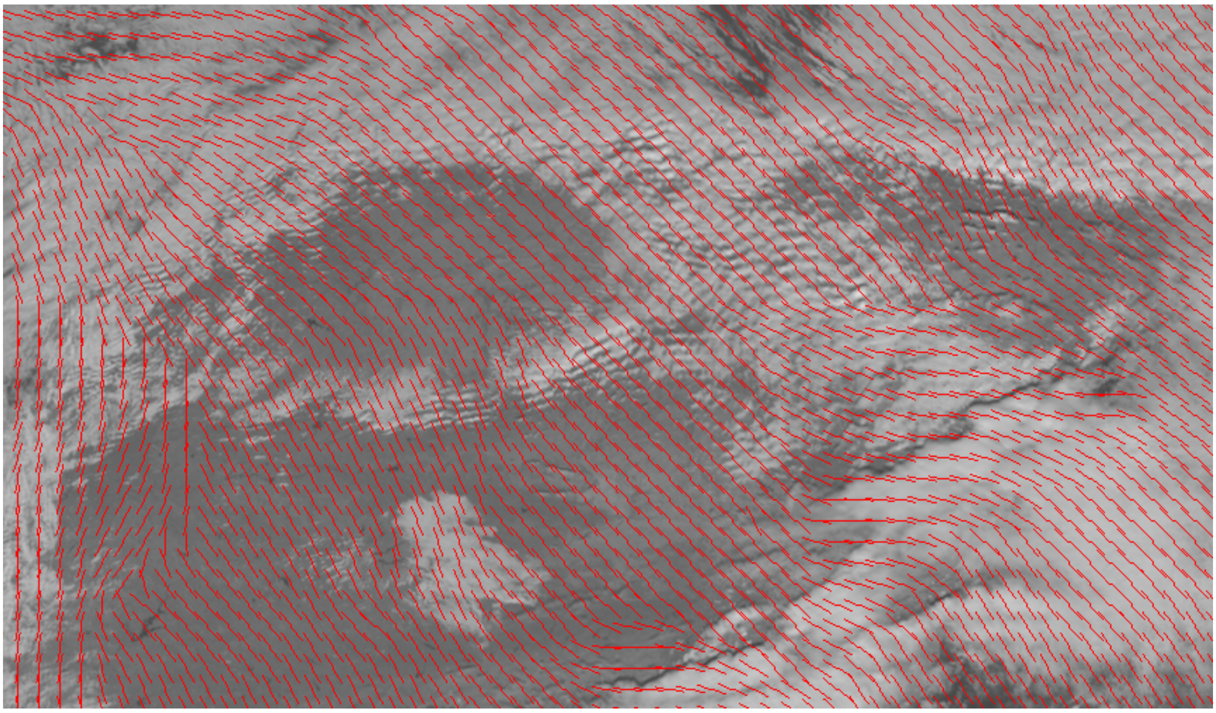

Figure 2: The red lines define the search area (pixel line) for the wave detection module. The user defined grid mesh distance is set to 15 satellite pixels. The direction of the lines is given by the interpolated HRW field.

At the time being, not all the envisaged input parameters have been tested in respect of their relevance for discriminating wave structures. Further candidates for testing are:

- The angle between the wind direction and the orientation of the mountain range
- A stability parameter (Showalter index), as atmospheric stability is one of the prerequisites for gravity waves to develop.

3.2 PRACTICAL CONSIDERATIONS

3.2.1 Validation

ASII-NG uses predefined criteria to detect regions favourable for turbulence, based primarily on satellite data. The absence of these criteria in the data does not automatically mean the absence of turbulence, since not all mechanisms of turbulence can be captured by ASII-NG. Thus it is not a fair measure of ASII-NG's performance to compare its detected fields of turbulence with actual fields of turbulence, since ASII-NG can only detect a subset of all turbulent fields. Validation of ASII-NG will therefore place more emphasis on the analysis of the structures detected. This means that validation will be (at least partly) subjective by checking if certain patterns which are commonly accepted as related to turbulence would be agreed by a meteorologist, too.

A verification of turbulence itself is very problematic. PIREPS (=pilot reports) could be used to check that areas recognized as being favourable for turbulence by ASII-NG were indeed found to be accompanied by turbulence. The problems with that method, however, are that PIREPS just deliver reports when turbulence is present. Furthermore, the reports are bound to flight routes, so that in regions without air traffic no verification can be given.

3.2.2 Quality control and diagnostics

In its current version, ASII-NG cannot provide results at pixels whose required input parameters are unavailable. The information regarding which input parameter(s) was/were missing is included as a separate flag field in the ASII-NG output file (field “asii_turb_trop_prob_status_flag”; cf. its more detailed description in ch. 3.2.3).

3.2.3 Description of the output

The ASII-NG product is encoded in a standard NWCSAF netCDF output file. As such, it features many standard entries/matrices common to all NWC/GEO netCDF products; such contents are described in the NWCSAF Data Output Format Document [RD.1]. There is one file per slot and it is located by default in $SAFNWC/export/ASII; the naming follows the schematic S_NWC_ASII-NG_MSG*i*_*<region>*-VISIR_*YYYYMMDD*T*hhmmss*Z.nc (example: S_NWC_ASII-NG_MSG3_global-VISIR_20150626T120000Z.nc).

Apart from the standard fields, the netCDF file holds the following ASII-NG-specific fields:

- “asii_turb_trop_prob”: derived probability for occurrence of tropopause folding; for each pixel a value between 0 and 100%, with failure to derive is at a certain pixel indicated by code 255.
- “asii_turb_trop_prob_status_flag”: giving more details on reasons why “asii_turb_trop_prob” could not be derived at a certain pixel. 0=everything OK, probability computed; otherwise:
    - bit 1 set: problem in “gradient in IR9.7”
    - bit 2 set: problem in “gradient in WV6.2”
    - bit 3 set: problem in ”gradient of the difference image IR9.7-IR10.8”
    - bit 4 set: problem in “shear vorticity” (NWP parameter)
    - bit 5 set: problem in “wind speed” (NWP parameter)
    - bit 6 set: problem in “tropopause from specific humidity” (NWP parameter that may require model levels in great height)
    - bit 7 set: problem in “tropopause from IPV” (NWP parameter that may require model levels in great height)
- asii_turb_prob_pal: a simple grayscale palette, stretching linearly over the 0-100 range
- the common processing conditions and quality flags (described in [RD.1]) for this product bear the names asiing_conditions and asiing_quality.

4. ASSUMPTIONS AND LIMITATIONS

The product is a satellite product which searches for structures favourable for turbulence but NOT the turbulence itself. This product is aimed to be one of the inputs for decision making by meteorologists and cannot be used as an stand-alone automatic warning tool.

As CAT by definition is a clear air phenomenon there may be areas of turbulence which cannot be detected by any remote sensing tool. In case of lee wave turbulence or transverse bandings, wave detection is limited to those cases where clouds form in the wave crest. In very dry areas the lifting of air parcels within the wave is not enough to initiate condensation. Therefore, the absence of signal in satellite imagery does not preclude the existence of CAT. In other words, even assuming the detection algorithm is working perfectly, the detection rate of CAT will never reach 1.

Although the NWCSAF software package can be processed at any region of the globe the focus of tuning and validation will be Europe and the neighbouring sea areas.

5. REFERENCES

Bader, M.J., Forbes, G.S., Grant, J.R., Lilley, R.B.E., and A.J. Waters (Eds.), 1995: Images in weather forecasting. Cambridge University Press, Cambridge.

Ellrod, G.P., and D.J. Knapp, 1991: An Objective Clear-Air Forecasting Technique: Verification and Operational Use, Weather and Forecasting, **7,** 150-165.

Ellrod, G.P., and J.A. Knox, 2010: Improvements to an Operational Clear-Air Turbulence Diagnostic Index by Addition of a Divergence Trend Term, Weather and Forecasting, **25,** 789–798. doi: http://dx.doi.org/10.1175/2009WAF2222290.1

Knox, J.A., McCann, D.W., and P.D. Williams, 2007: Application of the Lighthill–Ford Theory of Spontaneous Imbalance to Clear-Air Turbulence Forecasting, Journal of the Atmospheric Sciences, **65,** 3292–3304.

Lenz, A., 2008: Identification of Transverse Band Signature in Satellite Imagery, http://www.nwas.org/committees/rs/2008_MetSat_Papers/Lenz.pdf

McCann, D., 2001: Gravity Waves, Unbalanced Flow and Aircraft Clear Air Turbulence, National Weather Digest, **25,** 3-14.

Overeem, A., 2002: Verification of clear-air turbulence forecasts, Technisch rapport; TR-244, KNMI, De Bilt.

Sharman, R., Tebaldi, C., Wiener, G., and J. Wolff, 2006: An Integrated Approach to Mid- and Upper-Level Turbulence Forecasting, Weather and Forecasting, **21,** 268-287.

Uhlenbrock, N.L., Bedka, K.M., Feltz, W.F., and S.A. Ackerman, 2007: Mountain Wave Signatures in MODIS 6.7µm Imagery and Their Relation to Pilot Reports of Turbulence, Weather and Forecasting, **22,** 662-670.

Wimmers, A., and W. Feltz, 2010: Tropopause Folding Turbulence Product, Algorithm Theoretical Basis Document, UW/CIMSS, Version 2.0, May10, 2010. (http://www.goes-r.gov/products/ATBDs/option2/Aviation_Turbulence_v1.0_no_color.pdf).

World Meteorological Organization, 1978: Handbook of Meteorological Forecasting for Soaring Flights, WMO Technical Note Nr. 158.

ANNEX 1: ANCILLARY DATA

ASII-NG v1.0 makes use of the NWP fields of temperature, humidity and wind on all pressure levels listed in the central NWP configuration file (if available in the local GRIB file)